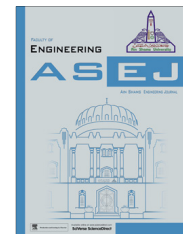




Ain Shams University

Ain Shams Engineering Journal

www.elsevier.com/locate/asej  
www.sciencedirect.com



## CIVIL ENGINEERING

# Prediction of scour caused by 2D horizontal jets using soft computing techniques

Masoud Karbasi <sup>a,\*</sup>, H. Md. Azamathulla <sup>b</sup>

<sup>a</sup> *Hydraulic Structures, Water Engineering Dep., Faculty of Agriculture, University of Zanjan, Zanjan, Iran*

<sup>b</sup> *Civil Engineering, Faculty of Engineering, University of Tabuk, Tabuk, Saudi Arabia*

Received 6 December 2015; revised 1 March 2016; accepted 9 April 2016

## KEYWORDS

2D horizontal jets;  
Scour hole;  
Sluice gate;  
Soft-computing

**Abstract** This paper presents application of five soft-computing techniques, artificial neural networks, support vector regression, gene expression programming, grouping method of data handling (GMDH) neural network and adaptive-network-based fuzzy inference system, to predict maximum scour hole depth downstream of a sluice gate. The input parameters affecting the scour depth are the sediment size and its gradation, apron length, sluice gate opening, jet Froude number and the tail water depth. Six non-dimensional parameters were achieved to define a functional relationship between the input and output variables. Published data were used from the experimental researches. The results of soft-computing techniques were compared with empirical and regression based equations. The results obtained from the soft-computing techniques are superior to those of empirical and regression based equations. Comparison of soft-computing techniques showed that accuracy of the ANN model is higher than other models ( $RMSE = 0.869$ ). A new GEP based equation was proposed.

© 2016 Faculty of Engineering, Ain Shams University. Production and hosting by Elsevier B.V. This is an open access article under the CC BY-NC-ND license (<http://creativecommons.org/licenses/by-nc-nd/4.0/>).

## 1. Introduction

Scour is a regular phenomenon of bringing down the riverbed level because of the evacuation of sediment by the erosive activity of a flowing stream. Local scour is produced close to the structures because of adjustment of the stream field as an

obstacle to the stream by the structures. Turbulent horizontal jets appear when flow is discharged through underflow gates and rectangular culverts [1].

The scour phenomenon downstream of a sluice gate is complex in nature due to rapid change of the flow characteristics on the sediment bed [2]. Local scour downstream of hydraulic structures by a jet issuing from a sluice gate has gotten impressive consideration in light of the fact that scour can jeopardize the foundation of the structure.

Laboratory study of scour downstream of sluice gates has been conducted by several researchers [2–16].

Dey and Sarkar [2] performed an experimental study on scour hole characteristics over a wide range of sediment size, tailwater depth, sluice opening and apron length and concluded the following results: The equilibrium scour depth,

\* Corresponding author. Tel.: +98 2433052388, +98 9123416540.

E-mail addresses: [m.karbasi@znu.ac.ir](mailto:m.karbasi@znu.ac.ir) (M. Karbasi), [mdazmath@gmail.com](mailto:mdazmath@gmail.com) (H. Md. Azamathulla).

Peer review under responsibility of Ain Shams University.



Production and hosting by Elsevier

<http://dx.doi.org/10.1016/j.asej.2016.04.001>

2090-4479 © 2016 Faculty of Engineering, Ain Shams University. Production and hosting by Elsevier B.V.

This is an open access article under the CC BY-NC-ND license (<http://creativecommons.org/licenses/by-nc-nd/4.0/>).

Please cite this article in press as: Karbasi M, Azamathulla HM, Prediction of scour caused by 2D horizontal jets using soft computing techniques, Ain Shams Eng J (2016), <http://dx.doi.org/10.1016/j.asej.2016.04.001>

**Notation**

$b$	gate opening
$d_{50}$	median sediment size
$e_i$	prediction error
$\bar{e}$	mean prediction error
$Fr_j$	jet Froude number
$g$	acceleration due to gravity
$h_t$	tailwater depth
$L_a$	apron length
$n$	number of data
$O_i$	observed value
$\bar{Q}_i$	mean value of observations
$P_i$	predicted value

$\bar{P}_i$	mean value of predictions
$R$	jet hydraulic radius
$S_e$	standard deviation of the prediction errors
$U$	velocity of jet
$w$	sediment fall velocity
$\rho$	mass density of water
$\rho_s$	mass density of sediments
$\mu_{A_i}(x)$	fuzzy membership function
$\nu$	kinematic viscosity of water
$\sigma_g$	sediment gradation

decreases with increase in sediment size and sluice opening. The equilibrium scour depth increases with rise in densimetric Froude number, and for a higher densimetric Froude number, the equilibrium scour depth is free of the densimetric Froude number. No uniformity of sediments decreases the scour depth downstream of the launching apron. Placing a launching apron decreases the scour depth.

Hamidifar et al. [9] examined the scour behaviors of the non-cohesive sediments downstream of smooth and rough aprons. The results showed that the principle attributes of the scour holes, such as the maximum scour depth and its distance from the end of the apron, the maximum extension of the hole, the dune height and its distance from the end of the apron, were much lower for rough than smooth aprons.

In spite of the reported experimental data sets, it is hard to thoroughly catch the impacts of the different parameters on the scour created in view of restrictions in the laboratory facilities and scope of tests that can be led. Thus, traditional methodologies utilizing regression-based techniques to predict the scour depth are regular. The empirical equations proposed by these procedures are fundamentally confined to the range of the database utilized in their derivation [17].

Recently, different artificial intelligence techniques such as artificial neural network (ANN) [18–29], adaptive neuron-fuzzy inference system (ANFIS) [20,30–38], support vector machine (SVM) [29,36,39–41], decision trees [22,41–44], genetic programming (GP) [45–47], linear genetic programming (LGP) [48,49], gene expression programming (GEP) [27,28,50], group method of data handling (GMDH), data mining [17,51–59], and machine learning method were utilized for modeling of problems in scour prediction.

Najafzadeh and Lim [17] developed structure of a neuro-fuzzy GMDH network as a self-organized method to estimate the scour depth downstream of a sluice gate with an apron. An evolutionary algorithm of PSO is developed with the NF-GMDH network for the training stage. The results indicated that the NF-GMDH-PSO network produced lower error in scour prediction than all other models.

This paper presents the modeling of local scour depth downstream of a sluice gate utilizing soft computing techniques: ANNs, SVR, GMDH, ANFIS and GEP. Results of soft computing techniques were compared with empirical and multiple regression based equations and finally a new GEP based equation was proposed.

**2. Methods***2.1. Theoretical background*

A definition sketch for local scour due to 2D horizontal jets is indicated in Fig. 1, which represents a typical condition of a local scour hole downstream from a sluice gate.

Local scour due to horizontal jets is influenced by the power of the jet, the size and uniformity of the bed material, the presence of an apron between the jet inlet and the erodible bed, and the tailwater depth. Most existing scour equations use gate opening as the major length scale for equilibrium local scour depth [1]. Maximum equilibrium scour depth downstream of a sluice gate, can be given in functional form as [2]:

$$D_s = \varphi(U, \rho, \rho_s, g, \nu, b, L_a, h_t, d_{50}, \sigma_g) \quad (1)$$

where  $U$  = issuing velocity of jet;  $\nu$  = kinematic viscosity of water;  $\rho$  = density of water;  $\rho_s$  = density of sediments;  $b$  = gate opening;  $g$  = gravitational acceleration;  $L_a$  = apron length;  $h_t$  = tailwater depth;  $d_{50}$  = median sediment size,  $\sigma_g$  = sediment gradation.

Applying the Buckingham  $\pi$  theorem, one gets

$$\frac{D_s}{b} = \psi\left(\frac{U}{\sqrt{gb}}, \frac{U \cdot b}{\nu}, \frac{\rho_s}{\rho}, \frac{L_a}{b}, \frac{d_{50}}{b}, \frac{h_t}{b}, \sigma_g\right) \quad (2)$$

The kinematic viscosity may not affect the scour depth in turbulent flow [60] and the ratio of  $\frac{\rho_s}{\rho}$  is constant and can be neglected. As a result the final equation is derived as follows:

$$\frac{D_s}{b} = \psi\left(\frac{U}{\sqrt{gb}}, \frac{L_a}{b}, \frac{d_{50}}{b}, \frac{h_t}{b}, \sigma_g\right) \quad (3)$$

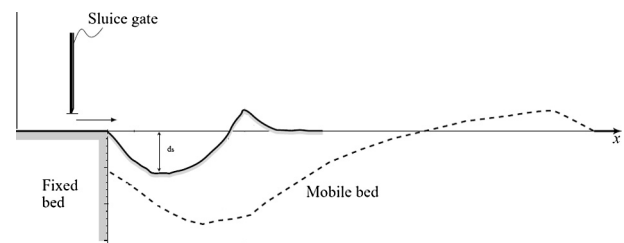


**Figure 1** Definition sketch for local scour due to 2D horizontal jets.

**Table 1** Laboratory data for scour depth caused by 2D horizontal jets issuing from sluice gates.

Researcher	Number of data	$D_s/b$	$Fr_j$	$h_t/b$	$d_{50}/b$	$L_a/b$	$\sigma_g$
Dey and Sarkar [2]	213	1.5–8.2	2.4–4.9	9.1–12.8	0.02–0.50	27–55	1.1–3.9
Aderibigbe and Rajaratnam [4]	32	1.3–32.7	1.2–21.5	6.9–60.0	0.05–1.35	0	1.3–3.1
Chatterjee et al. [7]	28	0.9–4.1	1.0–5.5	5.8–15.5	0.02–0.14	13–33	1.2–1.4

**Table 2** Descriptive statics of train and test data.

Variable	Data range		Mean		Standard deviation	
	Train	Test	Train	Test	Train	Test
$D_s/b$	0.6–24.4	0.5–21.7	12.5	11.10	3.20	3.87
$Fr_j$	1.23–21.54	1.02–17.43	11.38	9.22	2.36	2.71
$h_t/b$	3.66–65.73	5.7–65.73	34.7	35.72	11.17	13.54
$d_{50}/b$	0.017–1.35	0.015–1.35	0.684	0.683	0.198	0.204
$L_a/b$	0–60	0–60	30	30	12.75	14.00
$\sigma_g$	1–3.89	1–3.92	2.445	2.460	0.645	0.678

2.2. Available experimental data

A large number of experimental data for 2D horizontal jets have been published. The 273 laboratory data in Table 1 are utilized in the analysis presented in this paper. Statistical parameters of the train and test data are shown in Table 2. The training data were used for learning process and test data were used to evaluate the performance of the different models.

2.3. Experimental based empirical equations

Melville and Lim [1] analyzed 309 laboratory data for local scour depth and developed a new prediction equation.

$$\frac{D_s}{b} = 3Fr_j K_D K_{ht} K_\sigma K_L \tag{4}$$

where  $Fr_j$  is jet Froude number ( $U/\sqrt{gb}$ );  $K_D$  is sediment size effect:

$$K_D = 1 \text{ for } \frac{d_{50}}{b} < 0.6 \text{ and } K_D = 0.6 \left(\frac{d_{50}}{b}\right)^{-1} \text{ for } \frac{d_{50}}{b} \geq 0.6$$

$K_L$  is apron length effect:

$$K_L = 1 - \tanh\left(\frac{0.013L_a}{b}\right)$$

$K_{yt}$  is tailwater depth effect:

$$K_{ht} = 1 \text{ for } \frac{h_t}{b} > 6 \text{ and } K_D = 0.01 \left(\frac{h_t}{b}\right)^{2.6} \text{ for } \frac{h_t}{b} \leq 6$$

$K_\sigma$  is sediment gradation effect:

$$K_\sigma = 1 \text{ for } \sigma_g \leq 2.2 \text{ and } K_\sigma = 1.2\sigma_g^{-0.34} \text{ for } \sigma_g > 2.2$$

Selection of prediction equations for scour caused by 2D horizontal jets has been presented in Table 3.

2.4. Regression analysis

One of the traditional issues in statistical analysis is to discover a suitable relationship between a feedback variable and a set of input variables. Regression analysis is normally used to portray quantitative connections between a feedback variable and one or more informative variables. In MLR, the function is a linear mathematical statement, i.e. straight-line, in the form:

$$Y = a_0 + a_1 X_1 + a_2 X_2 + \dots + a_n X_n \tag{5}$$

where  $Y$  is the response variable,  $a_0$ – $a_n$  are the equation parameters for the linear equation, and,  $X_1$ – $X_n$  are the independent variables [61].

Multiple nonlinear regression (MNLr) is a manifestation of regression analysis in which observational information is modeled by a function, which is a nonlinear combination of the model parameters and relies on one or more independent

**Table 3** Selection of prediction equations for scour depth downstream of sluice gate.

Researcher	Equation
Dey and Sarkar [2]	$\frac{D_s}{b} = 2.59(Fr_{dj})^{0.94} \left(\frac{h_t}{b}\right)^{0.16} \left(\frac{L_a}{b}\right)^{-0.37} \left(\frac{d_{50}}{b}\right)^{0.25} Fr_{dj} = \frac{U_j}{[(S_G-1)gd_{50}]^{0.5}}$
Lim and Yu [11]	$\frac{D_s}{b} = 1.04(Fr_{dj})^{1.47} \left(\frac{d_{50}}{b}\right)^{0.33} \sigma_g^{-0.69} K_L K_L = \exp\left[-0.004(Fr_{dj})^{-0.35} \sigma_g^{-0.5} \left(\frac{d_{50}}{b}\right)^{-0.5} \left(\frac{L_a}{b}\right)^{1.4}\right]$
Chatterjee et al. [7]	$\frac{D_s}{b} = 0.775Fr_j$
Ali and Lim [5]	$\frac{D_s}{R} = 2.3(Fr_{dj})^{0.75} \left(\frac{U_j}{w}\right)^{0.5} \left(\frac{d_{50}}{R}\right)^{0.375} - 1.19$ where $R$ = jet hydraulic radius; and $w$ = sediment fall velocity
Altinbilek and Basmaci [6]	$\frac{D_s}{b} = \left(\frac{b}{d_{50}} \tan\phi\right)^{0.5} (Fr_{dj})^{1.5}$

variables [62]. Dissimilar to customary MLR, which is limited to estimating linear models, MNLR can estimate models with nonlinear relationships between input and response variables. The general presentation of the nonlinear relation is assumed to be the following:

$$Y = b_0 X_1^{b_1} \cdot X_2^{b_2} \dots X_n^{b_n} \quad (6)$$

where  $b_0$ – $b_n$  are the equation parameters.

### 2.5. Artificial neural network

Artificial neural networks as the most well-known artificial intelligence models are an accumulation of neurons with particular structure formed based on the relationship between neurons in different layers [63]. Neuron is a mathematical unit, and an artificial neural network that comprises of neurons is a complex and nonlinear framework. A static ANN known as a multilayer perceptron (MLP) is the most applied ANN in distinctive fields of engineering. Application of the artificial neural networks in the field of water resources and hydraulic engineering has grown quickly in the recent decade [63]. An ANN typically comprises of three layers: the input layer, where the data are introduced to the network; the hidden layer or layers, where data are processed; and the output layer, where the results of given input are produced [64]. A multi-layer feed-forward back-propagation neural network with one hidden (median) layer has been used in the present study [65]. In a feed-forward back-propagation neural network, the weighted connections feed activations only in the forward direction from an input layer to the output layer. These interconnections are adjusted utilizing an error convergence technique so that the network's response best matches the desired response. The major superiority of the ANN technique over conventional methods is that it does not require information about the complex nature of the process [64].

In this study one hidden layer including 5 neurons was used for the neural networks model. Too few neurons give a poor fit on unseen data, while too many neurons result in over-training of the net on the training set. Back-propagation algorithm was used as a training algorithm in this study.

### 2.6. Support vector regression

Classification of data is a routine task in data-driven modeling. Utilizing support vector machines, we can apart classes of data by a hyper plane. A support vector machine (SVM) is a concept for a set of related supervised learning methods that analyze data and recognize patterns, used for classification and regression analysis [63]. Support vector machine was developed by Vapnik in 1995 [66]. The basic difference between the application of SVM for regression (SVR) and the application of SVM for classification is that in SVR output is considered as a real number instead of a binary number [63]. The detail computation procedure can be found in [66].

### 2.7. Adaptive Neuro-Fuzzy Inference System

Adaptive Neuro-Fuzzy Inference Systems were developed by Jung in 1993. Neuro-fuzzy model combines artificial neural network (ANN) and fuzzy inference system (FIS) to facilitate the process of learning and adaptation. In neuro-fuzzy models, a

multilayer feed forward neural network is used to identify the parameters of an adaptive network fuzzy inference system. Importantly, fuzzy logic allows the communication between the input space and output space with a list of If-then sentences, called law. Having a method that uses the data to construct these rules is considered as an efficient tool. On the other hand, capabilities of artificial neural networks for training, using different educational models can establish the relationship between input and output variables. Therefore, the combination of fuzzy inference system and artificial neural network as a powerful tool that can predict the results of numerical data is available, as adaptive neuro-fuzzy inference system is introduced. This system of neural networks and fuzzy logic algorithms is used to design nonlinear mapping between input and output spaces.

ANFIS consists of five layers (Fig. 2):

*Layer 1:* input nodes. Each node of this layer creates membership grades based on the proper fuzzy set they belong to using membership functions. The node output  $O_{1,i}$  is defined by the following:

$$O_{1,i} = \mu_{A_i}(x) \quad \text{for } i = 1, 2$$

$$O_{1,i} = \mu_{B_{i-2}}(x) \quad \text{for } i = 3, 4$$

where  $x$  (or  $y$ ) is the input to the node, and  $A_i$ , (or  $B_{i-2}$ ) is a fuzzy set associated with this node, characterized by the shape of the membership functions in this node and can be any suitable functions that are continuous and piecewise differentiable such as Gaussian, generalized bell shaped, trapezoidal shaped and triangular shaped functions [64]. In this research, the generated bell-shaped membership function with below-mentioned equation was utilized:

$$\mu_{A_i} = \frac{1}{1 + \left| \frac{x-c_i}{a_i} \right|^{2b_i}} \quad \mu_{B_{i-2}} = \frac{1}{1 + \left| \frac{x-c_i}{a_i} \right|^{2b_i}} \quad (7)$$

where  $a_i$ ,  $b_i$  and  $c_i$  are the parameters of the membership functions in the premise part of fuzz If-Then rules that alter the shapes of the membership function with the maximum equal to 1 and the minimum equal to 0, and  $(a_i, b_i, c_i)$  are called premise parameters [64].

*Layer 2:* rule nodes. Each node in this layer multiplied by the input signal and output is result of all the input signals:

$$O_{2,i} = w_i = \mu_{A_i}(x) \times \mu_{B_{i-2}}(x), \quad i = 1, 2 \quad (8)$$

*Layer 3:* Average nodes. Each node of this layer which was named  $N$ , calculates the ratio of normalized rules:

$$O_{3,i} = \bar{w} = \frac{w_i}{w_1 + w_2}, \quad i = 1, 2 \quad (9)$$

*Layer 4:* Consequent nodes. Node  $i$  in this layer calculates the contribution of the  $i$ th rule toward the model output, with the following function:

$$O_{4,i} = \bar{w}_i f = \bar{w}_i (p_i + q_i + r_i), \quad i = 1, 2 \quad (10)$$

where  $\bar{w}$  is the output of the layer 3 and  $(p_i, q_i, r_i)$  is the consequent parameter set.

*Layer 5:* Output nodes. The single node in this layer calculates the overall output of the ANFIS which is non-fuzzy as follows:

$$O_{5,i} = \sum_{i=1}^4 \bar{w}_i f = \frac{\sum_{i=1}^4 w_i f}{\sum_{i=1}^4 w_i} \quad (11)$$

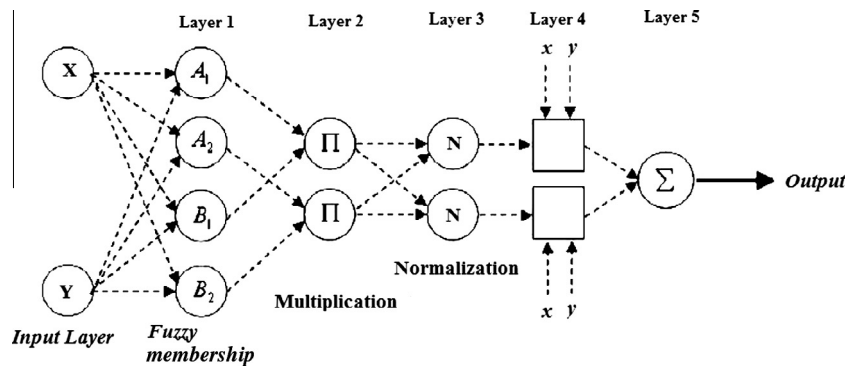


Figure 2 Structure of ANFIS [64].

In this research, the hybrid learning algorithm, which combines the least-squares method and the back-propagation, is utilized to train and adapt the FIS.

More detailed information about ANFIS can be found in Jang [67].

2.8. Gene Expression Programming

Gene Expression Programming (GEP) is a new evolutionary Artificial Intelligence method developed by Ferreira [68]. This Method is an extension of GP, developed by Koza [69]. All three algorithms (GA, GP and GEP) are part of the wider class of genetic algorithms as all of them use populations of individuals, select the individuals according to fitness, and introduce genetic variation using one or more genetic operators [70]. The main difference between the three algorithms resides in the nature of the individuals: in GAs the individuals are symbolic strings of constant length (chromosomes); in GP the individuals are nonlinear entities of different dimensions and shapes (parse trees); and in GEP the individuals are also nonlinear entities of different dimensions and shapes (expression trees), but these complicated entities are encoded as simple strings of constant length [70]. GEP is a full-fledged genotype/phenotype system, with the genotype totally detached from the phenotype, while in GP, genotype and phenotype are one embroiled mess or more formally, a simple replicator system. As a result, the full-fledged genotype/phenotype system of GEP surpasses the elderly GP system by a factor of 100–60,000 [71].

2.9. GMDH Neural Networks

GMDH Neural Network is a self-organizing approach by which more complicated models are gradually generated based on the evaluation of their performance on a set of multi-input, single-output data pairs [72]. This approach was proposed by Ivakhnenko in the 1960s. It has a series of operations, such as seeding, rearing, crossbreeding, and selection and rejection of seeds corresponding to the determination of the input variables, the structure and parameters of the model, and the selection of the model by the principle of termination [72].

The typical GMDH algorithm can be represented as a set of neurons in which different pairs of them in each layer are connected through a quadratic polynomial and thus produce new neurons in the next layer [73]. General connection between

inputs and output variables can be expressed by a complicated discrete form of the Volterra functional series in the form of [74]:

$$y = a_0 + \sum_{i=1}^m a_i x_i + \sum_{i=1}^m \sum_{j=1}^m a_{ij} x_i x_j + \sum_{i=1}^m \sum_{j=1}^m \sum_{k=1}^m a_{ijk} x_i x_j x_k + \dots \tag{12}$$

which is known as the Kolmogorov–Gabor polynomial, where  $X = (x_1, x_2, \dots, x_m)$  is the input vector, and  $y$  is the output variable. GMDH works by building successive layers with complex links that are the individual terms of a polynomial. The initial layer is simply the input layer. The first layer created is made by computing regressions of the input variables and then choosing the best ones. The second layer is created by computing regressions of the values in the first layer along with the input variables. This means that the algorithm essentially builds polynomials of polynomials [75]. More detail on mathematical background of GMDH Neural Network can be found in the literature [17,36,51–59].

2.10. Performance evaluation criteria

To estimate the accuracy of the proposed models the following expressions were used:

$$RMSE = \sqrt{\frac{\sum_{i=1}^N (O_i - P_i)^2}{N}} \tag{13}$$

$$MBE = \frac{1}{N} \sum_{i=1}^N (O_i - P_i) \tag{14}$$

$$MAE = \frac{1}{N} \sum_{i=1}^N |O_i - P_i| \tag{15}$$

$$MAPE = \frac{1}{N} \sum_{i=1}^N \left| \frac{O_i - P_i}{O_i} \right| \tag{16}$$

$$R^2 = \frac{(\sum_{i=1}^N (O_i - \bar{O}_i)(P_i - \bar{P}_i))^2}{\sum_{i=1}^N (O_i - \bar{O}_i)^2 \sum_{i=1}^N (P_i - \bar{P}_i)^2} \tag{17}$$

where  $O_i$  is the observed value,  $P_i$  is the predicted value,  $\bar{O}_i$  is the mean value of observations,  $\bar{P}_i$  is the mean value of predictions,  $i$  is the subscript which indicates the ID of data, and  $N$  is the total number of data. The  $RMSE$  describes the average difference between predicted value and measured value. Mean average error ( $MAE$ ) shows how developed models overesti-

mate or underestimate the measured values. Mean average percentage error (*MAPE*) describes the accuracy of the models by error percentage. The coefficient of determination  $R^2$  describes the degree of association between the predicted and the measured values.

### 3. Results and discussion

At the present study, in order to predict the scour depth downstream of a sluice gate, ANN, SVR, ANFIS and GEP methods were used. The results of the models were compared with the regression models and empirical equations.

#### 3.1. Multiple Linear Regression

A multiple linear regression analysis of the experimental data (Table 1) yields the following equation of non-dimensional equilibrium scour depth downstream of an apron due to submerged jets issuing from a sluice opening:

$$\frac{D_s}{b} = 1.151 + 1.253Fr_j - 3.371 \frac{d_{50}}{b} - 0.497\sigma_g + 0.057 \frac{h_t}{b} - 0.032 \frac{l_a}{b} \quad (18)$$

#### 3.2. Multiple nonlinear regression

A multiple nonlinear regression analysis of the experimental data yields the following equation of non-dimensional equilibrium scour depth downstream of a sluice gate:

$$\frac{D_s}{b} = 0.626Fr_j^{1.05} \frac{d_{50}^{-0.273} h_t^{0.0165}}{b} \sigma_g^{0.668} \quad (19)$$

#### 3.3. Artificial neural network

In this research, a multi-layer perceptron neural network with one hidden layer and back-propagation training algorithm was used. The parameters of BP algorithm were adopted as follows: the learning rate = 0.05, initial maximum number of epochs = 10,000, momentum constant = 0.95 and minimum performance gradient =  $1e-15$ . To determine number of neurons at hidden layer trial and error method was applied. To do this 2–20 neurons were tested at hidden layer. Results showed that minimum *RMSE* occurs at 4 neurons at hidden layer. The  $R^2$  of this model is higher than those of other MLP models. As a result, the MLP model having 4 hidden neurons in hidden layer was selected as the best fit model for scour depth prediction. Fig. 3 shows the results with the performance indices between predicted and observed data for the training and testing data sets, respectively. Fig. 3 shows that the MLP model performance is accurate and reliable. As can be seen from Fig. 3b, the MLP model underestimates the maximum scour depth for test data.

#### 3.4. ANFIS model

In the ANFIS model, fuzzy subtractive clustering algorithm was used to design an initial rule base. The objective of the fuzzy subtractive clustering was to prevent increasing numbers

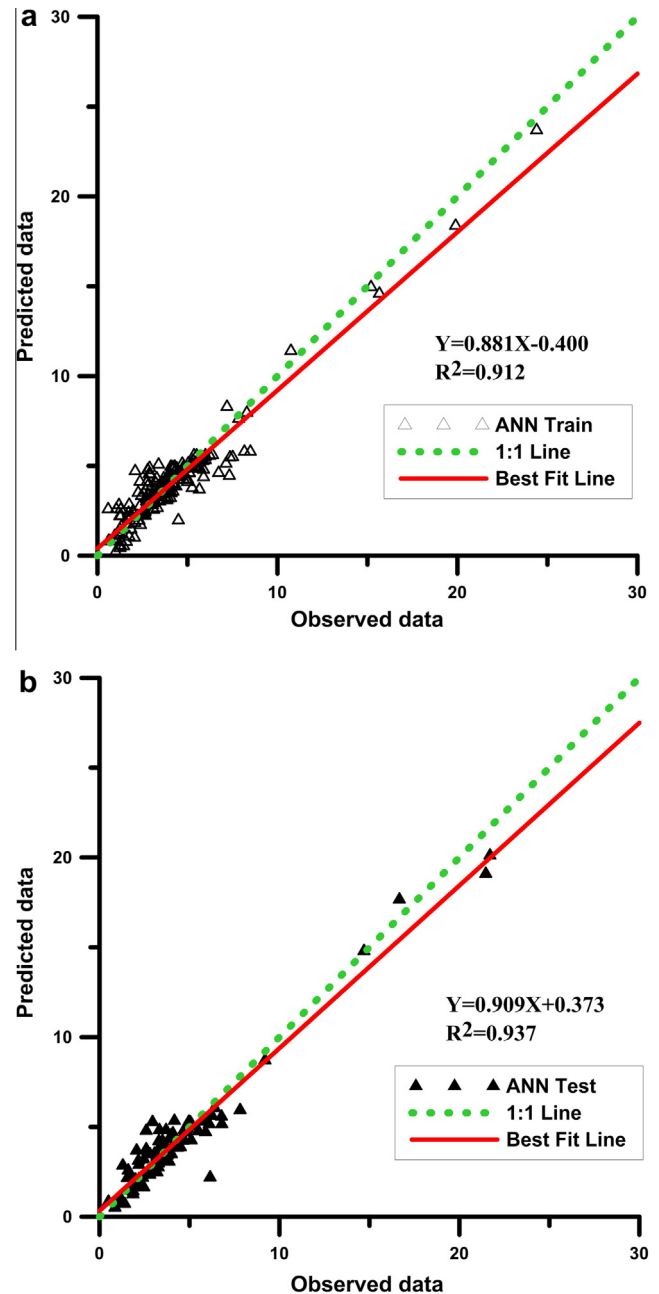
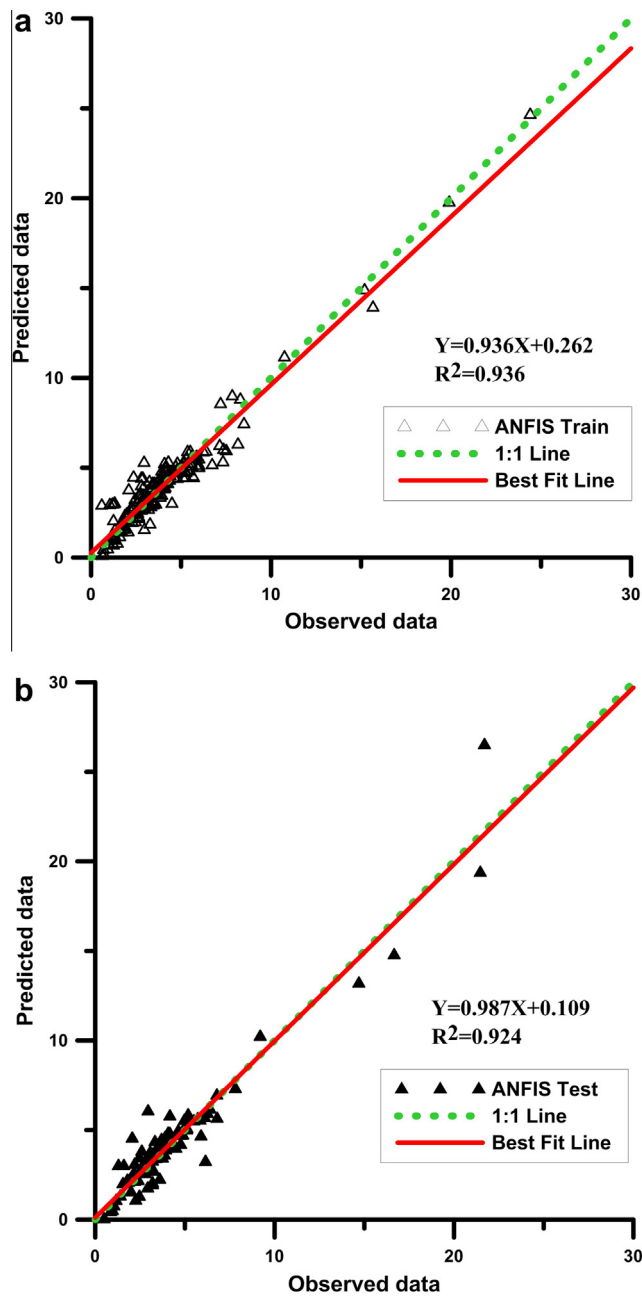


Figure 3 Plot of observed and predicted scour depth with original data set using ANN model (a) training and (b) test.

of parameters which may be altered according to the number of rules. The *genfis2* function generates a model from data using clustering and requires a specified cluster radius. Specifying a small cluster radius usually yields many small clusters in the data hence resulting in many rules. Specifying a large cluster radius usually yields a few large clusters in the data which results in fewer rules. Cluster size 0.5 was chosen for the test as it shows a satisfaction of training and testing result. A combination of least-squares method and back-propagation algorithm (hybrid model) is used to optimize the function parameters.

To evaluate the performance of the ANFIS model, observed dimensionless scour depth values are plotted against



**Figure 4** Plot of observed and predicted scour depth with original data set using ANFIS model (a) training and (b) test.

the predicted ones. Fig. 4 shows the results with the performance indices between predicted and observed data for the training and testing data sets, respectively. As can be seen from Fig. 4 ANFIS has performed well in predicting the dimensionless scour depth.

### 3.5. SVR model

Fig. 5 provides the graph plotted between observed and predicted value of dimensionless scour depth obtained by using RBF kernel based SVR with the train and test data. As can be seen from Fig 5b, the SVR model overestimates the maximum scour depth for test data.

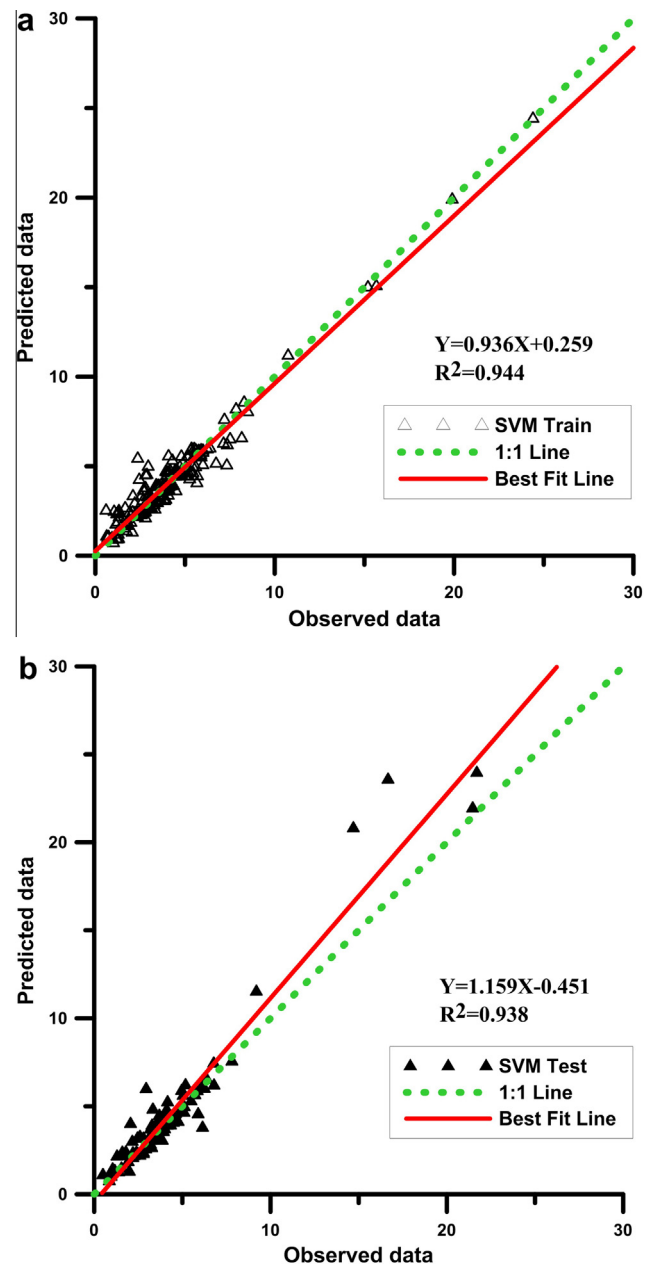


**Figure 5** Plot of observed and predicted scour depth with original data set using SVR model (a) training and (b) test.

### 3.6. GEP model

The chromosomal architecture including number of chromosomes (30-50-100), head size (2-4-7) and number of genes (2-3-5) were selected and different combination of the mentioned parameters was tested. The model was run for number of generations and was stopped when there was no significant change in the fitness function value and coefficient of correlation. After some trials, it was found that after 40,000 generations, there was no appreciable change. Parameters of the optimized GEP model are shown in Table 4.

The explicit formulations of GEP for non-dimensional scour depth prediction as a function of  $\frac{U}{\sqrt{g_b}}$ ,  $\frac{L_a}{b}$ ,  $\frac{d_{50}}{b}$ ,  $\frac{h_i}{b}$ ,  $\sigma_g$  were obtained as follows:

**Table 4** Parameters of the optimized GEP model.

Parameters	Definition	Value
$P_1$	Function set	$+, -, \div, \times, x^n, pow(x, y), sinh, tanh, Ln, In v$
$P_2$	Mutation rate	0.044
$P_3$	Inversion rate	0.1
$P_4$	One-point recombination rate	30%
$P_5$	Two-point recombination rate	30%
$P_6$	Gene recombination rate	0.1
$P_7$	Gene transposition rate	0.1
$P_8$	Linking function	Addition
$P_9$	Fitness function	RMSE

$$\frac{D_s}{b} = a_1 + a_2 + a_3 \tag{20}$$

$$a_1 = \tanh \left[ \left( 2.75 Fr_j \cdot \left( \frac{d_{50}}{b} \right)^{1/5} \right) - \left( \frac{L_a}{b} \frac{d_{50}}{b} + \sigma_g \frac{L_a}{b} \right) \right] \tag{21}$$

$$a_2 = \left| \sinh \left( \frac{d_{50}}{b} \right) + \left( \frac{Fr_j}{\tanh(Fr_j - 8.689)} \right) \right| \tag{22}$$

$$a_3 = \ln(Fr_j) * \left[ \frac{1}{\left( (1.51 \frac{d_{50}}{b}) (\frac{L_a}{b} + \sigma_g) \right)^{1/3}} \right] \tag{23}$$

Fig. 6 provides the graph plotted between observed and predicted value of dimensionless scour depth obtained by using GEP model with the train and test data set. Fig. 7 shows the expression trees of the aforesaid formulation.

### 3.7. GMDH Neural Network

A two-variable quadratic polynomial function was used in this study. Back propagation algorithm used to train the network. Fig. 8 provides the graph plotted between observed and predicted value of dimensionless scour depth obtained by using GMDH Neural Network with the train and test data set.

### 3.8. Comparison soft-computing methods and empirical equations

To assess the performance of different soft-computing methods, results of the soft-computing methods are compared with empirical models. Table 5 indicates the statistical parameters for different models for test and train data set. According to Table 5, almost all of the soft-computing techniques perform better than regression and empirical based models for test data. ANN model is the best model for prediction of dimensionless scour depth ( $RMSE = 0.839$ ,  $R^2 = 0.955$  for train data and  $RMSE = 0.869$ ,  $R^2 = 0.937$  for test data). The second best model is GEP model ( $RMSE = 0.761$ ,  $R^2 = 0.962$  for train data and  $RMSE = 0.957$ ,  $R^2 = 0.961$  for test data). After GEP model, GMDH, ANFIS and SVM models estimate the maximum scour depth by  $RMSE = 0.964$ ,  $0.971$  and  $1.175$  respectively. ANFIS, GMDH and SVM models overestimate the maximum scour depth for test data ( $MBE = -0.052$ ,  $-0.01$  and  $-0.231$  respectively), while ANN and GEP models underestimate it ( $MBE = 0.076$  and  $0.015$  respectively). The main advantage of the GEP model is an algebraic equation

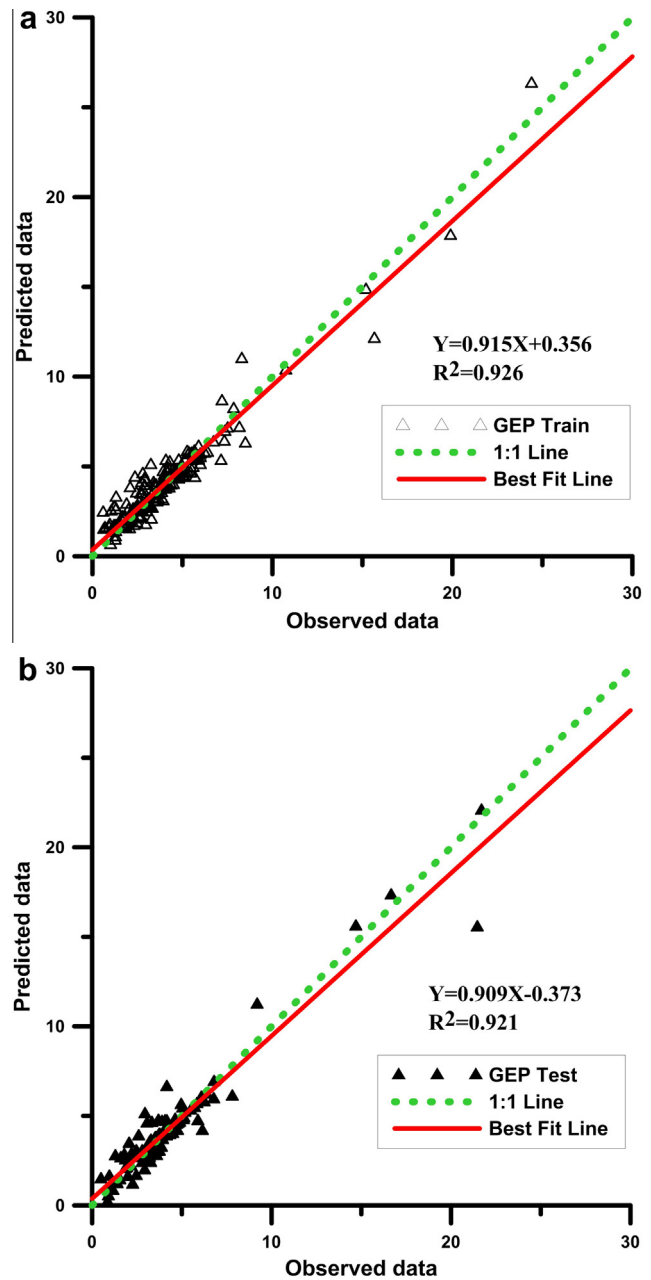


**Figure 6** Plot of observed and predicted scour depth with original data set using GEP model (a) training and (b) test.

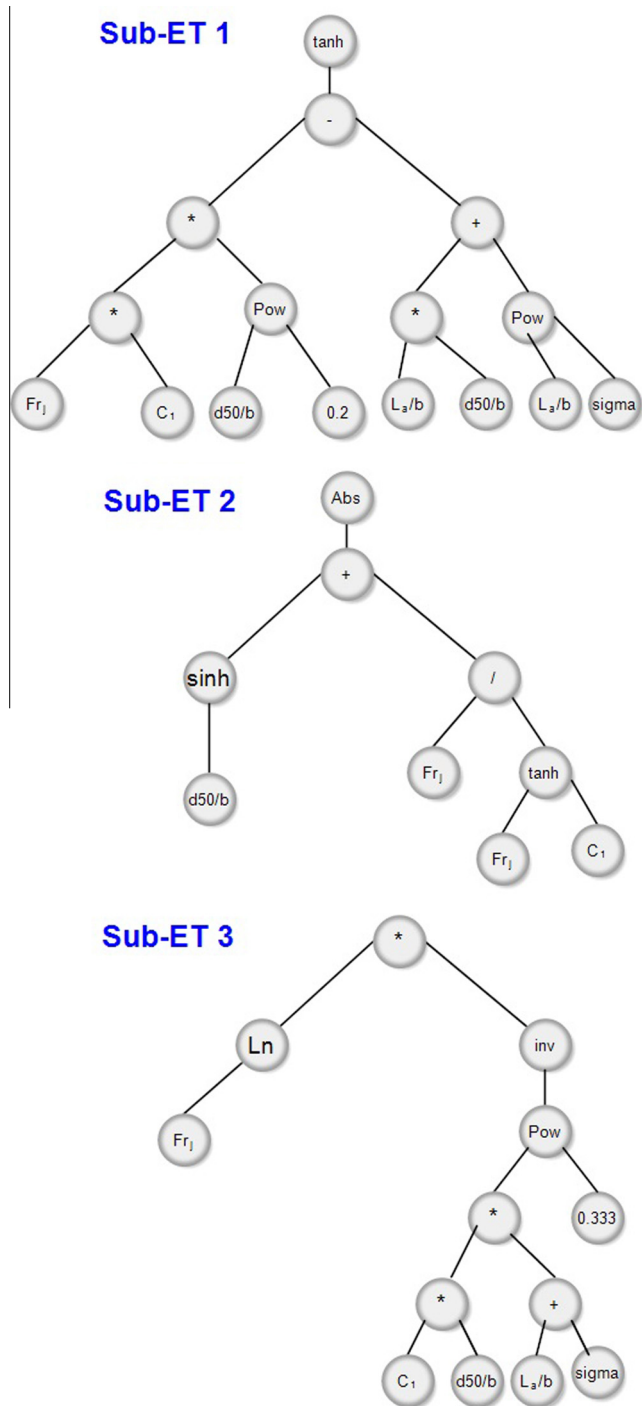


Figure 7 GEP expression tree.

that can be used easily for practical applications. The GMDH model predicts the values of dimensionless scour depth by  $RMSE = 0.799$ ,  $R^2 = 0.958$  for train data and  $RMSE = 0.964$ ,  $R^2 = 0.966$  for test data.

As can be seen from Table 5, the equation suggested by Dey and Sarkar [2] ( $RMSE = 1.048$ ,  $R^2 = 0.937$ ) provides better estimation than other empirical equations. Linear and nonlinear regression equations (Eqs. (18) and (19)) proposed in the present study could not increase the accuracy of Dey and

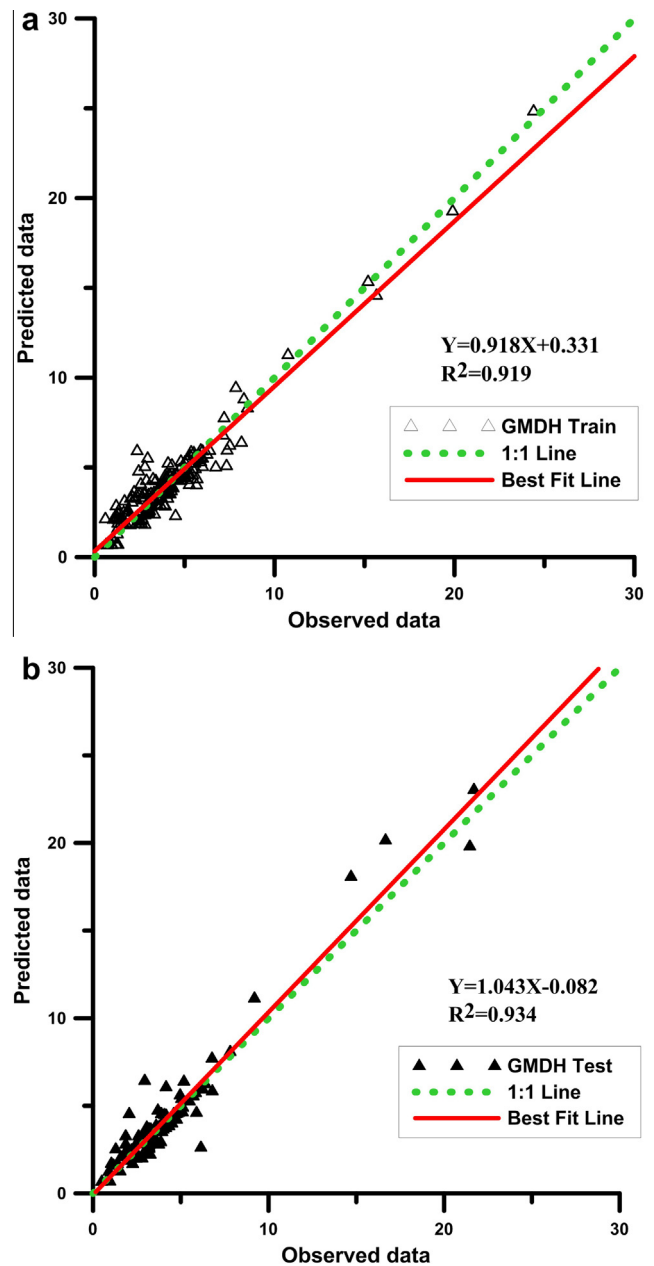


Figure 8 Plot of observed and predicted scour depth with original data set using GMDH model (a) training and (b) test.

Sarkar [2] equation ( $RMSE = 1.266$  for linear regression and  $RMSE = 2.324$  for nonlinear regression). Empirical equations suggested by Melville and Lim [1], Lim and Yu [11] and Chatterjee et al. [7] had lower accuracy ( $RMSE = 3.419$ ,  $RMSE = 2.136$  and  $RMSE = 2.278$  respectively). Dey and Sarkar [2], Lim and Yu [11] and Melville and Lim [1] equations overestimate the maximum scour depth ( $MBE = -0.417$ ,  $-0.851$  and  $-2.525$  respectively), while Chatterjee et al. [7] underestimate the maximum scour depth ( $MBE = 1.457$ ). Melville and Lim [1] equation had the worst accuracy and mean averaged percentage error ( $MAPE$ ) was about 80%. Thus, in comparison with other models and equations, application of this equation is not recommended.

**Table 5** Performance of different models for train and test data sets.

Model	RMSE	MBE	MAPE %	MAE	R <sup>2</sup>
ANN (test)	<b>0.869</b>	0.076	18.842	0.615	0.968
SVM (test)	1.175	-0.231	<b>15.78</b>	<b>0.601</b>	0.968
ANFIS (test)	0.971	-0.052	19.42	0.626	<b>0.971</b>
GEP (test)	0.957	0.015	20.04	0.602	0.961
GMDH (test)	0.964	<b>-0.010</b>	17.94	0.621	0.966
ANN (train)	0.839	0.085	20.67	0.599	0.955
SVM (train)	<b>0.661</b>	<b>0</b>	<b>17.52</b>	<b>0.469</b>	<b>0.972</b>
ANFIS (train)	0.711	<b>0</b>	19.25	0.509	0.967
GEP (train)	0.761	-0.011	20.14	0.538	0.962
GMDH (train)	0.799	<b>0</b>	21.51	0.594	0.958
Nonlinear multiple regression	2.324	-0.768	43.73	1.307	0.832
Linear multiple regression	1.266	0.449	29.386	0.955	0.938
Melville and Lim [1]	3.419	-2.525	80.471	2.541	0.925
Dey and Sarkar [2]	1.048	-0.417	36.919	0.727	0.937
Lim and Yu [11]	2.136	-0.851	37.607	1.172	0.915
Chatterjee et al. [7]	2.278	1.457	34.313	1.594	0.896

Bold values are best results.

**Table 6** Sensitivity analysis for input parameters with ANN model.

Function	R <sup>2</sup> (train)	RMSE (train)	R <sup>2</sup> (test)	RMSE (test)
$\frac{D_s}{b} = \psi \left( \frac{U}{\sqrt{gb}}, \frac{L_a}{b}, \frac{d_{s0}}{b}, \frac{h_t}{b} \right)$	0.892	0.924	0.908	1.549
$\frac{D_s}{b} = \psi \left( \frac{L_a}{b}, \frac{d_{s0}}{b}, \frac{h_t}{b}, \sigma_g \right)$	0.527	2.029	0.731	<b>1.793</b>
$\frac{D_s}{b} = \psi \left( \frac{U}{\sqrt{gb}}, \frac{d_{s0}}{b}, \frac{h_t}{b}, \sigma_g \right)$	0.919	0.806	0.885	1.444
$\frac{D_s}{b} = \psi \left( \frac{U}{\sqrt{gb}}, \frac{L_a}{b}, \frac{d_{s0}}{b}, \sigma_g \right)$	0.865	1.521	0.843	1.621
$\frac{D_s}{b} = \psi \left( \frac{U}{\sqrt{gb}}, \frac{L_a}{b}, \frac{h_t}{b}, \sigma_g \right)$	0.844	1.124	0.857	1.333

Bold values are best results.

3.9. Sensitivity analysis

To evaluate the significance of input variables on maximum scour depth, sensitivity analysis was performed on the ANN model due to minimum error of it. In the analysis, one parameter of Eq. (3) was eliminated each time to assess its affection to the output. In this way, the RMSE values are characterized as common statistical errors. Results of sensitivity analysis are presented in Table 6. Accordingly, the jet Froude number ( $Fr_{d_j}$ ) was found to be the most effective parameter ( $R^2 = 0.731$ ,  $RMSE = 1.793$ ) on the prediction of maximum scour depth. While the apron length ratio ( $L_a/b$ ) was found to be the least effective parameter on the prediction of maximum scour depth. Aderibigbe and Rajaratnam [4] also showed that the scour depth is primarily a function of the jet desimetric Froude number.

4. Conclusion

In this paper an attempt was made to determine the best method for estimating maximum scour depth issuing from a sluice gate. The results of the ANN, ANFIS, SVR and GEP methods had good agreements with the measured experimental data. Also the results of these models were compared with the existing empirical [1,2,7,11] and regression based equations. Data sets for performing the training and testing stages were gathered from literatures [2,4,7]. It was shown that the ANN, SVR, ANFIS, GMDH and GEP models had less computational errors than the empirical equations. Moreover results showed that soft computing models are superior to regression models (linear and nonlinear). The rank of soft computing models according to root mean square error was ANN, GEP, GMDH, ANFIS and SVM ( $RMSE = 0.869$ ,  $0.957$ ,  $0.964$ ,  $0.971$  and  $1.175$  respectively). Comparing GEP and ANN methods, derived equation from GEP is more applicable than the black box approach of ANN; however, the accuracy of ANN model was slightly higher than GEP model. Between the traditional equations, Dey and Sarkar [2] equation had relatively low errors ( $RMSE = 1.048$  and  $MAPE = 36.9\%$ ) in comparison with other equations. Melville and Lim [1] equation did not yield satisfactory results for data set of the present study ( $RMSE = 3.419$  and  $MAPE = 80.4\%$ ). Additionally, sensitivity analysis is performed and it is found that Jet Froude number is the most effective parameter on maximum scour depth downstream of a sluice gate. On the other hand, apron length ratio is the least effective parameter on maximum scour depth. For the future researchers it is proposed that meta-heuristic optimization techniques such as particle swarm optimization (PSO) and artificial bee colony (ABC) are applied for training process of soft computing techniques.

References

- [1] Melville B, Lim S. Scour caused by 2D horizontal jets. *J Hydraul Eng* 2014;140(2):149–55.
- [2] Dey S, Sarkar A. Scour downstream of an apron due to submerged horizontal jets. *J Hydraul Eng* 2006;132(3):246–57.
- [3] Valentin F. Considerations concerning scour in the case of flow under gates; 1967.
- [4] Aderibigbe O, Rajaratnam N. Effect of sediment gradation on erosion by plane turbulent wall jets. *J Hydraul Eng* 1998;124(10):1034–42.
- [5] Ali K, Lim S. Local scour caused by submerged wall jets. In: *ICE Proceedings*. Thomas Telford; 1986.
- [6] Altinbilek HD, Basmaci Y. Localized scour at the downstream of outlet structures. In: *Proc. 11th congress on large dams*.
- [7] Chatterjee S, Ghosh S, Chatterjee M. Local scour due to submerged horizontal jet. *J Hydraul Eng* 1994;120(8):973–92.
- [8] Farhodi J, Smith KV. Time scale for scour downstream of hydraulic jump. *J Hydraul Div* 1982;108(10):1147–62.
- [9] Hamidifar H, Omid M, Nasrabadi M. Scour downstream of a rough rigid apron. *World Appl Sci J* 2011;14(8):1169–78.
- [10] Hopfinger EJ et al. Sediment erosion by Görtler vortices: the scour-hole problem. *J Fluid Mech* 2004;520:327–42.
- [11] Lim S, Yu G. Scouring downstream of sluice gate. In: *First international conference on scour of foundations*.
- [12] Verma DVS, Goel A. Scour downstream of a sluice gate. *ISH J Hydraul Eng* 2005;11(3):57–65.

- [13] Balachandar R, Kells JA, Thiessen RJ. The effect of tailwater depth on the dynamics of local scour. *Can J Civ Eng* 2000;27(1):138–50.
- [14] Farhoudi J, Smith KVH. Local scour profiles downstream of hydraulic jump. *J Hydraul Res* 1985;23(4):343–58.
- [15] Balachandar R, Kells JA. Instantaneous water surface and bed scour profiles using video image analysis. *Can J Civ Eng* 1998;25(4):662–7.
- [16] Balachandar R, Kells JA. Local channel in scour in uniformly graded sediments: the time-scale problem. *Can J Civ Eng* 1997;24(5):799–807.
- [17] Najafzadeh M, Lim S. Application of improved neuro-fuzzy GMDH to predict scour depth at sluice gates. *Earth Sci Inf* 2014;1–10.
- [18] Ayoubloo MK, Etemad-Shahidi A, Mahjoobi J. Evaluation of regular wave scour around a circular pile using data mining approaches. *Appl Ocean Res* 2010;32(1):34–9.
- [19] Azamathulla HM, Deo MC, Deolalikar PB. Alternative neural networks to estimate the scour below spillways. *Adv Eng Softw* 2008;39(8):689–98.
- [20] Bateni SM, Borghei SM, Jeng DS. Neural network and neuro-fuzzy assessments for scour depth around bridge piers. *Eng Appl Artif Intell* 2007;20(3):401–14.
- [21] Bateni SM, Jeng D-S, Melville BW. Bayesian neural networks for prediction of equilibrium and time-dependent scour depth around bridge piers. *Adv Eng Softw* 2007;38(2):102–11.
- [22] Etemad-Shahidi A, Yasa R, Kazeminezhad MH. Prediction of wave-induced scour depth under submarine pipelines using machine learning approach. *Appl Ocean Res* 2011;33(1):54–9.
- [23] Firat M, Gungor M. Generalized regression neural networks and feed forward neural networks for prediction of scour depth around bridge piers. *Adv Eng Softw* 2009;40(8):731–7.
- [24] Ismail A et al. Predictions of bridge scour: application of a feed-forward neural network with an adaptive activation function. *Eng Appl Artif Intell* 2013;26(5–6):1540–9.
- [25] Kaya A. Artificial neural network study of observed pattern of scour depth around bridge piers. *Comput Geotech* 2010;37(3):413–8.
- [26] Lee TL et al. Neural network modeling for estimation of scour depth around bridge piers. *J Hydrodyn Ser B* 2007;19(3):378–86.
- [27] Moussa YAM. Modeling of local scour depth downstream hydraulic structures in trapezoidal channel using GEP and ANNs. *Ain Shams Eng J* 2013;4(4):717–22.
- [28] Onen F. Prediction of scour at a side-weir with GEP, ANN and regression models. *Arab J Sci Eng* 2014;39(8):6031–41.
- [29] Ghazanfari-Hashemi S et al. Prediction of pile group scour in waves using support vector machines and ANN. *J Hydroinform* 2011;13(4):609–20.
- [30] Farhoudi J, Hosseini SM, Sedghi-Asl M. Application of neuro-fuzzy model to estimate the characteristics of local scour downstream of stilling basins. *J Hydroinform* 2010;12(2):201–11.
- [31] Akib S, Mohammadhassani M, Jahangirzadeh A. Application of ANFIS and LR in prediction of scour depth in bridges. *Comput Fluids* 2014;91:77–86.
- [32] Azamathulla HM, Ghani AAb, Fei SY. ANFIS-based approach for predicting sediment transport in clean sewer. *Appl Soft Comput* 2012;12(3):1227–30.
- [33] Bateni SM, Jeng DS. Estimation of pile group scour using adaptive neuro-fuzzy approach. *Ocean Eng* 2007;34(8–9):1344–54.
- [34] Keshavarzi A, Gazni R, Homayoon SR. Prediction of scouring around an arch-shaped bed sill using neuro-fuzzy model. *Appl Soft Comput* 2012;12(1):486–93.
- [35] Zounemat-Kermani M et al. Estimation of current-induced scour depth around pile groups using neural network and adaptive neuro-fuzzy inference system. *Appl Soft Comput* 2009;9(2):746–55.
- [36] Najafzadeh M, Etemad-Shahidi A, Lim SY. Scour prediction in long contractions using ANFIS and SVM. *Ocean Eng* 2016;111:128–35.
- [37] Firat M. Scour depth prediction at bridge piers by Anfis approach. *Proc Inst Civ Eng – Water Manage* 2009;162(4):279–88.
- [38] Firat M, Gungör M. Monthly total sediment forecasting using adaptive neuro fuzzy inference system. *Stoch Environ Res Risk Assess* 2009;24(2):259–70.
- [39] Goel A, Pal M. Application of support vector machines in scour prediction on grade-control structures. *Eng Appl Artif Intell* 2009;22(2):216–23.
- [40] Hong J-H et al. Predicting time-dependent pier scour depth with support vector regression. *J Hydrol* 2012;468–469:241–8.
- [41] Goyal MK, Ojha CSP. Estimation of scour downstream of a ski-jump bucket using support vector and M5 model tree. *Water Resour Manage* 2011;25(9):2177–95.
- [42] Etemad-Shahidi A, Ghaemi N. Model tree approach for prediction of pile groups scour due to waves. *Ocean Eng* 2011;38(13):1522–7.
- [43] Samadi M, Jabbari E, Azamathulla HM. Assessment of M5' model tree and classification and regression trees for prediction of scour depth below free overfall spillways. *Neural Comput Appl* 2012;24(2):357–66.
- [44] Pal M, Singh NK, Tiwari NK. M5 model tree for pier scour prediction using field dataset. *KSCE J Civ Eng* 2012;16(6):1079–84.
- [45] Guven A, Gunal M. Genetic programming approach for prediction of local scour downstream of hydraulic structures. *J Irrig Drain Eng* 2008;134(2):241–9.
- [46] Azamathulla HMD et al. Genetic programming to predict ski-jump bucket spill-way scour. *J Hydrodyn Ser B* 2008;20(4):477–84.
- [47] Azamathulla HMD et al. Genetic programming to predict bridge pier scour. *J Hydraul Eng* 2009;136(3):165–9.
- [48] Azamathulla HM, Guven A, Demir YK. Linear genetic programming to scour below submerged pipeline. *Ocean Eng* 2011;38(8–9):995–1000.
- [49] Guven A, Azamathulla HM, Zakaria NA. Linear genetic programming for prediction of circular pile scour. *Ocean Eng* 2009;36(12–13):985–91.
- [50] Azamathulla H, Yusoff MAMohd. Soft computing for prediction of river pipeline scour depth. *Neural Comput Appl* 2013;23(7–8):2465–9.
- [51] Najafzadeh M. Neuro-fuzzy GMDH based particle swarm optimization for prediction of scour depth at downstream of grade control structures. *Eng Sci Technol Int J* 2015(0).
- [52] Najafzadeh M, Barani GA. Comparison of group method of data handling based genetic programming and back propagation systems to predict scour depth around bridge piers. *Sci Iran* 2011;18(6):1207–13.
- [53] Najafzadeh M, Barani G-A, Azamathulla HM. GMDH to predict scour depth around a pier in cohesive soils. *Appl Ocean Res* 2013;40:35–41.
- [54] Najafzadeh M, Barani G-A, Hessami Kermani MR. GMDH based back propagation algorithm to predict abutment scour in cohesive soils. *Ocean Eng* 2013;59:100–6.
- [55] Najafzadeh M, Barani G-A, Hessami-Kermani M-R. Evaluation of GMDH networks for prediction of local scour depth at bridge abutments in coarse sediments with thinly armored beds. *Ocean Eng* 2015;104:387–96.
- [56] Najafzadeh M, Azamathulla HM. Neuro-fuzzy GMDH to predict the scour pile groups due to waves. *J Comput Civ Eng* 2015;29(5):04014068.
- [57] Najafzadeh M. Neurofuzzy-based GMDH-PSO to predict maximum scour depth at equilibrium at culvert outlets. *J Pipeline Syst Eng Pract* 2016;7(1):06015001.

- [58] Najafzadeh M, Barani G-A, Hessami-Kermani M-R. Group method of data handling to predict scour at downstream of a ski-jump bucket spillway. *Earth Sci Inf* 2014;7(4):231–48.
- [59] Najafzadeh M. Neuro-fuzzy GMDH systems based evolutionary algorithms to predict scour pile groups in clear water conditions. *Ocean Eng* 2015;99:85–94.
- [60] Rajaratnam N. Erosion by plane turbulent jets. *J Hydraul Res* 1981;19(4):339–58.
- [61] Tabari H et al. SVM, ANFIS, regression and climate based models for reference evapotranspiration modeling using limited climatic data in a semi-arid highland environment. *J Hydrol* 2012;444–445:78–89.
- [62] Bilgili M. Prediction of soil temperature using regression and artificial neural network models. *Meteorol Atmos Phys* 2010;110(1–2):59–70.
- [63] Araghinejad S. *Data-driven modeling: using MATLAB in water resources and environmental engineering*. Springer; 2014.
- [64] Wang W-C et al. A comparison of performance of several artificial intelligence methods for forecasting monthly discharge time series. *J Hydrol* 2009;374(3–4):294–306.
- [65] Hykin S. *Neural networks: a comprehensive foundation*. New Jersey: Printice-Hall. Inc.; 1999.
- [66] Vapnik V. *The nature of statistical learning theory*. Springer; 1995.
- [67] Jang JSR. ANFIS: adaptive-network-based fuzzy inference system. *IEEE Trans Syst Man Cybernet* 1993;23(3):665–85.
- [68] Ferreira C. Gene expression programming: a new adaptive algorithm for solving problems. arXiv: preprint cs/0102027; 2001.
- [69] Koza JR. *Genetic programming: on the programming of computers by means of natural selection*, vol. 1. MIT press; 1992.
- [70] Ferreira C. *Gene expression programming*. Berlin: Springer; 2006.
- [71] Zakaria NA et al. Gene expression programming for total bed material load estimation—a case study. *Sci Total Environ* 2010;408(21):5078–85.
- [72] Garg V. Inductive group method of data handling neural network approach to model basin sediment yield. *J Hydrol Eng* 2014;20(6):C6014002.
- [73] Nariman-zadeh N et al. Modelling of explosive cutting process of plates using GMDH-type neural network and singular value decomposition. *J Mater Process Technol* 2002;128(1–3):80–7.
- [74] Kalantary F, Ardalan H, Nariman-Zadeh N. An investigation on the Su–NSPT correlation using GMDH type neural networks and genetic algorithms. *Eng Geol* 2009;104(1–2):144–55.
- [75] Witczak M et al. A GMDH neural network-based approach to robust fault diagnosis: application to the DAMADICS benchmark problem. *Control Eng Pract* 2006;14(6):671–83.



**Dr. Masoud Karbasi** is Assistant Professor in Department of water engineering, Faculty of Agriculture, University of Zanjan, Islamic Republic of Iran, He graduated in irrigation Engineering from the Urmia University in 2003 and post graduated in Hydraulic Structure from University of Tehran in 2005. He completed his PhD in Hydraulic Structures from University of Tehran in 2011. He has published 4 Journal papers; presented more than 15 conferences papers. His interest research is hydraulics of sediment transport, river engineering and hydraulic structures.



**Dr. H.Md. Azamathulla** is Associate Professor in Department of civil engineering, Faculty of Engineering, University of Tabuk, Saudi Arabia, He graduated in Civil Engineering from the S. K. D., University, Ananthapur in 1994 and post graduated from SGSITS, Devi Ahilya University, Indore in 1997. He completed his PhD from Indian Institute of Technology, Bombay in 2005.